BUT

CO$_2$ Separation from Syngas by Multiwall Carbon Nanotube

Soodabeh Khalili, Ali Asghar Ghoreyshi and Mohsen Jahanshahi

Department of Chemical Engineering, Babol University of Technology, Babol, Iran

Abstract: In this study the equilibrium uptakes of hydrogen and carbon dioxid as the main constituents of syngas by the multi-walled carbon nanotube (MWCNT) were investigated at the temperature range of 288-318 K and pressure up to 40 bars. The results have shown that temperature had much less effect on the adsorption of H$_2$ on MWCNT than adsorption of CO$_2$. Several model isotherms such as Langmuir and Freundlich were examined to fit the equilibrium uptake data. The kinetics of H$_2$ and CO$_2$ adsorption on MWCNT were also investigated and the results revealed a fast sorption kinetic for both gas adsorption on MWCNT. Isosteric heat of adsorption was evaluated based on the Clausius-Clapeyron equation at different temperatures. Small values of isosteric heat of adsorption confirmed that although the adsorption of H$_2$ and CO$_2$ on MWCNT were exothermic, but the heat of adsorption was too low, therefore the process of adsorption of both gases on the MWCNT used in this study is physisorption.

Key words: Syngas · Adsorption · MWCNT · Kinetic · Isosteric heat

INTRODUCTION

Hydrogen has recently attracted a great deal of attention as a clean energy source in view of decreasing fossil fuel supply [1, 2]. A primary current technology or hydrogen generation is by coal gasification that produces synthesis gases containing mainly H$_2$, CO and CO$_2$. In order to produce additional hydrogen, CO is converted in to H$_2$ and CO$_2$ in the water gas shift (WGS) reactor [3, 4]. To gain hydrogen with high purity, it should be separated CO$_2$ from H$_2$.

Several methods have been proposed to capture CO$_2$, including chemical absorption, physical absorption, cryogenic separation, physical adsorption and membrane separation [5-7]. Among them, chemical absorption with aqueous solution of alkanolamines has been recognized as the most common process. However, solvent absorption technology has several drawbacks such as high corrosion, oxidative degradation of absorbents, high-energy consumption for solvent regeneration, high viscosity and foaming in the gas-liquid interface [8, 9]. To overcome these problems, physical adsorption with porous materials has received increasing attention for CO$_2$ capture from flue gas. Many types of porous media have been developed such as molecular sieves, zeolite, activated carbon, etc. to adsorb and store gases [10-12]. Among solid adsorbents, carbonaceous materials have been evaluated as a potential adsorbent in CO$_2$ separation. Some interesting properties of these materials such as high surface area, large pore volume and low density render them as suitable materials for high gas adsorption [13, 14]. Since the discovery of carbon nanotube (CNT) by Iijima in 1991 [15], many researchers have examined the adsorption property of this new kind of material. These materials have unique properties such as uniform porosity, high specific surface area, low mass density [16]. The internal and external adsorption sites of the curved nanotubes increased the adsorption surface; therefore the extent of adsorption has occurred [17]. Recently, Pressure swing adsorption (PSA) processes using porous adsorbents have become one of promising candidates for CO$_2$ adsorption due to low cost, high selectivity, high adsorption capacity and easy regeneration of adsorbents [18]. Having knowledge of the

Corresponding Author: Soodabeh Khalili, Department of Chemical Engineering, Babol University of Technology, Babol, Iran.

adsorption isotherms is the first step in the design of a PSA system. Equilibrium parameters are also required as input information to the modeling and simulation of PSA processes. The adsorption isotherms give an insight about maximum gas storage capacity attainable by a specific adsorbent [19].

The main objective of the present research was to assess the potential of MWCNT as an effective adsorbent for capture of CO_2 from syngas. Experimental results of gas adsorption by MWCNT at equilibrium state were described by several model isotherms. The kinetic study was also carried out to evaluate the effectiveness of the adsorption processes. Isosteric heat of adsorption was evaluated from a set of isotherms based on the Clausius-Clapeyron equation.

MATERIALS AND METHODS

Material and its Characterization: The MWCNT used in this work were purchased from Alpha Nanotechnologies Company, Ltd (China) which was synthesized with chemical vapor deposition (CVD) method. Carbon dioxide, hydrogen and helium with purity of 99.99%, 99.999% and 99.995% respectively, were purchased from Technical Gas Services, UAE.

MWCNT were characterized by scanning electron microscopy (SEM) by using TESCAN VegaII model microscope to obtain supplementary information about the MWCNT structure. With SEM in combination, the EDX (Energy Dispersive X-ray spectroscopy) is used as an analytical technique to find out which elements different parts of a MWCNT contain. The physical properties of MWCNT were measured by BET technique

(Belsorp mini II model manufactured by BelJapan Company) employing N_2 adsorption isotherm at 77K. N_2 adsorption/desorption isotherms were determined at a relative pressure (P/P_0) range of 0.0001-0.99 and used to measure surface area, average pore diameter and pore volume.

Apparatus: The amount of adsorbed hydrogen and carbon dioxide on the MWCNT were determined by volumetric technique. Fig. 1 displays the apparatus that was designed to conduct the gas adsorption experiments.

The apparatus was consisted of two high-pressure cells made of stainless steel, called as pressure and adsorption cell. They were placed in a thermostatic water bath (with working temperature range of 283-363K manufactured by Merck Company) to keep the temperature constant during the gas adsorption. The pressure cell was connected to a regulator and adsorption cell via a needle valve to control gas entrance. Gas flew from gas high-pressure reservoir to the pressure cell via the regulator (1) by opening the connecting valve (2). The adsorption experiments were initiated by opening the valves 5 and 6 between pressure cell and adsorption cell and allowing gas entrance to the adsorption cell loaded with the adsorbent. The pressure in the system was started to drop as gas was adsorbed on the adsorbent. The equilibrium state was reached when the pressure approached to a constant value. Both cells equipped with a PT100 temperature probe and a pressure transducer that were interfaced to the computer to monitor and record system pressure. The maximum allowable pressure in the installation was 50 bars and its working temperature was in the range of 283-343K.
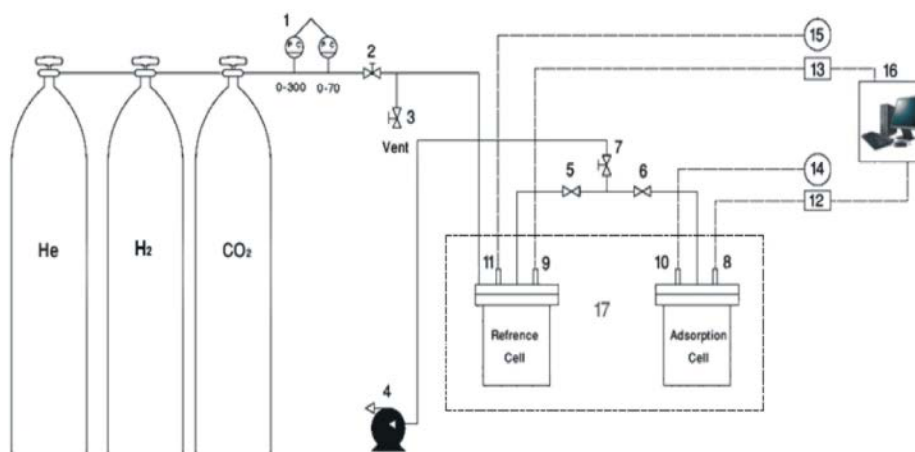

Fig. 1: Schematic diagram of the volumetric adsorption apparatus: (1) regulator; (2,3) needle valves; (4) vacuum pump; (5,6) ball valves; (7) needle valve; (8,9) pressure transducer; (10,11) temperature probe; (12,13) pressure digital indicator; (14,15) temperature digital indicator; (16) computer; (17) water bath

Prior loading adsorbent into the adsorption cell, the setup was tested against any probable leak using pressurized air for 24 hours. Before each test, the adsorbent was degassed at 473K for 24 hours and the system was evacuated by vacuum pump to 0.1 mbar. Also the He gas was employed to determine the dead volume by using a calibration cell with a definite volume. By this method the exact volume of pressure and adsorption cell with their connection lines such as tubes and valves were measured.

The amount of adsorbed H_2 and CO_2 was calculated using material balance before and after each test and SRK equation of state for the compressibility factor:

$$\left.\frac{PV}{ZRT}\right|_{L_1} + \left.\frac{PV}{ZRT}\right|_{a_1} = \left.\frac{PV}{ZRT}\right|_{L_2} + \left.\frac{PV}{ZRT}\right|_{a_2} + N \qquad (1)$$

Where subscripts 1, 2, L and a stand for the initial state, final equilibrium state, pressure cell and adsorption cell, respectively. Also V is the volume, P is the pressure, T is the temperature, R is the universal gas constant and Z is the gas compressibility factor.

RESULT AND DISCUSSION

Materials Characterizations: The textural properties such as BET surface area, pore diameter and pore volume were listed in Table 1. Also elements different parts of MWCNT measured by SEM-EDX analysis were shown in Table 1. The N_2 adsorption and desorption isotherms at 77K of the MWCNT is shown in Fig. 2.

The SEM image for MWCNT was shown in Fig. 3. It is obvious due to their very short length, pristine-MWCNTs showed a little degree of entanglement. There are gray fragments in the structure of MWCNT, which indicates that MWCNTs contain many impurities almost amorphous carbon and carbonaceous particles. Short lengths of this type of MWCNT caused to increase of BET surface area. The short length of MWCNT maybe occurred during purification of CNT with concentrated acids.

H_2 and CO_2 Adsorption Isotherms: At any constant temperature, the amount of gas adsorbed on adsorbent is only a function of the pressure. By increasing pressure
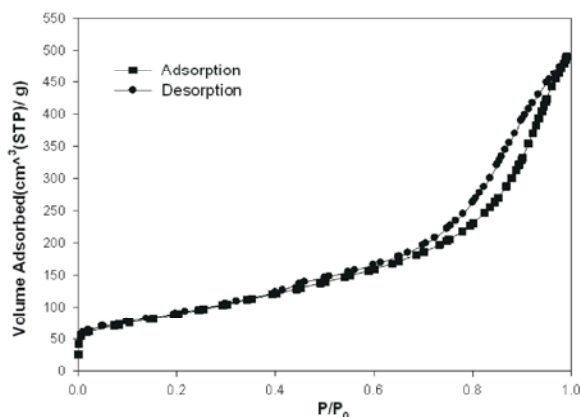

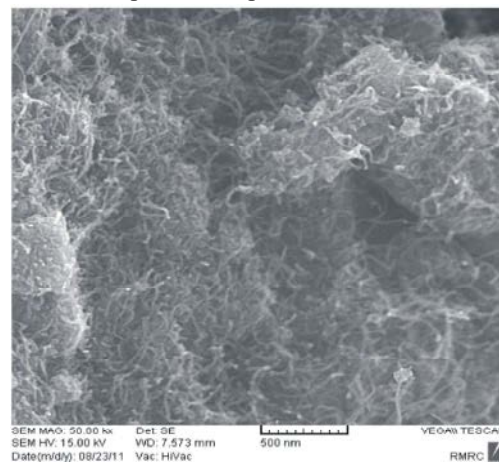Fig. 2: N_2 adsorption/desorption isotherms of MWCNT

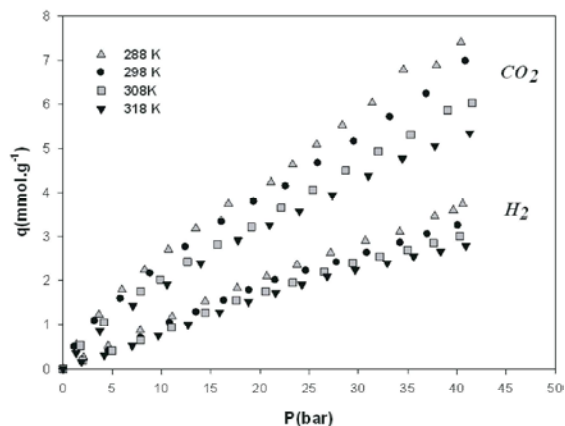Fig. 3: SEM image of MWCNT used in this study

Fig. 4: The variation in equilibrium uptake of H_2 and CO_2 by MWCNT with pressure

Table 1: Technical data of the MWCNT

Elemental analysis (%)						
C	O	Impurity (Ca)	Impurity (Au)	S_{BET} (m²/g)	Pore volume (cm³/g)	Mean pore diameter (nm)
89.50	7.76	0.25	2.49	324	0.76	9.36

Table 2: Langmuir and Freundlich isotherm constants for adsorption of H_2 and CO_2 on MWCNT.

| | H₂ | | | | | | CO₂ | | | | | |
| | Langmuir | | | Freundlich | | | Langmuir | | | Freundlich | | |
T(K)	q_m	K_L	R^2	K_F	n	R^2	q_m	K_L	R^2	K_F	n	R^2
288	16.125	0.0072	0.9997	0.1539	1.1674	0.9994	20.77	0.0132	0.9932	0.428	1.3022	.9974
298	15.04	0.0069	0.9989	0.1302	1.1417	0.9974	19.31	0.0129	0.9928	0.3945	1.3067	0.9980
308	13.96	0.0069	0.9987	0.1201	1.1387	0.9969	17.82	0.0121	0.9960	0.3334	1.2865	0.9992
318	12.36	0.0073	0.9977	0.1126	1.1433	0.9952	13.97	0.0148	0.9985	0.3268	1.3261	0.9997

and decreasing temperature, uptake of gases increased (Fig. 4). Results indicated that temperature had much less effect on the adsorption of H_2 on MWCNT than adsorption of CO_2 at the temperature range under study. Also the amount of CO_2 adsorption on MWCNT is about two times higher than H_2 adsorption may be attributed to this fact that the mean pore diameter of this sample is almost higher than H_2 molecule size compared with CO_2 molecule. The existence of the impurity in this MWCNT decreased the number of available sites for gas adsorption. Therefore, upon removal of impurities such as amorphous carbon and metal catalyst, attached to the surface of CNTs, larger outer surface is exposed to gas, improving gas adsorption capacity [20, 21].

The amount of adsorbed material onto an adsorbent as a function of its pressure at constant temperature can be described by different adsorption isotherm models. Adsorption on CNTs follows the Langmuir isotherm model which is based on three key assumptions that adsorption cannot proceed beyond monolayer coverage, adsorption sites equivalence and sites independence [22]. The Langmuir isotherm is given in the following equation:

$$q_e = q_m \frac{K_l P}{1 + K_l P} \qquad (2)$$

Where q_e is the amount of gas adsorbed per unit mass of MWCNT (mmol.g^{-1}); q_m is the maximum amount of gas adsorbed (mmol.g^{-1}) and K_L is $K_L = K_a/K_b$, K_a and K_b are adsorption and desorption constants, respectively.

The Freundlich model is an empirical equation which is used for non ideal sorption on heterogeneous surfaces and it is not restricted to the monolayer sorption [23]. Freundlich adsorption isotherm is given by:

$$q_e = k_F P^{\frac{1}{n}} \qquad (3)$$

Where K_F is Freundlich constant and $1/n$ is the heterogeneity factor. For n >1, adsorption is favorable. The Freundlich isotherm indicates reversible adsorption process [24, 25].
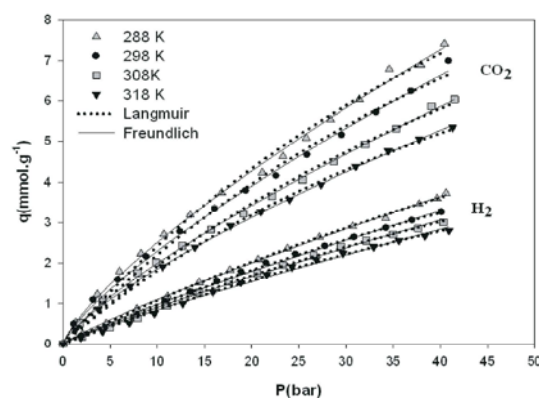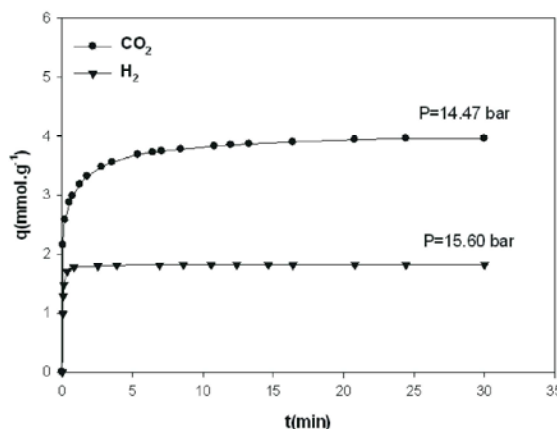

Fig. 5: Nonlinear fit of experimental data with Langmuir and Freundlich models

Fig. 6: Kinetics of H_2 and CO_2 adsorption by MWCNT at 288 K

The isotherm parameters were obtained through a nonlinear fit of experimental data with isotherm models by using SigmaPlot software. Fig. 5 shows the comparison of experimental adsorption data to predicted values by Langmuir and Freundlich isotherm models. The obtained values of Langmuir and Freundlich isotherm parameters are shown in Table 2.

The maximum gas capacity (q_m) for adsorption and K_L values decreased with increasing temperature. These results confirm that the affinity between CO_2 and H_2 on
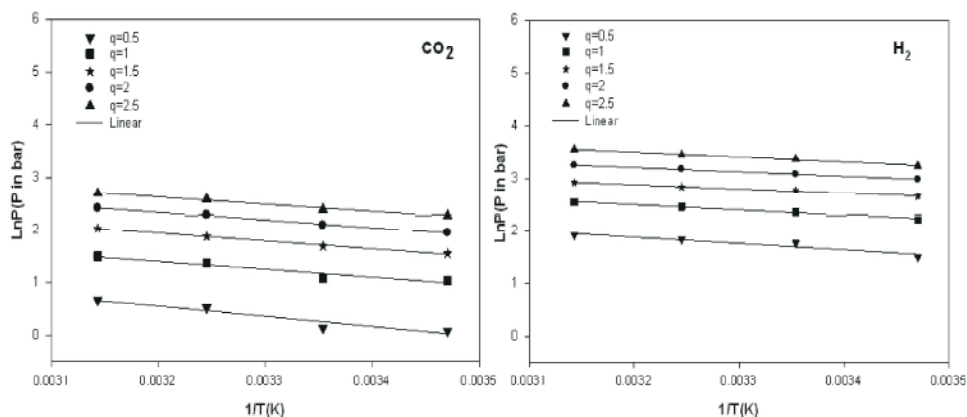
Fig. 7: Isosteric heat of adsorption of H_2 and CO_2 on the MWCNT (q in mmol.g^{-1})

MWCNT had an inverse relationship with temperature and indicating an exothermic reaction [26]. The n values of the Freundlich isotherm equation are more than 1, so adsorption is favorable. The K_F value of the gas adsorbed by the MWCNT decreased when temperature increased. These results suggested that the adsorption of the both gases on these sorbent is more favorable at low temperature [27].

H_2 and CO_2 Adsorption Kinetics: Kinetic studies of adsorption are necessary to evaluate the effectiveness of an adsorption process. By this way it could be to predict the rate-limiting step in an adsorption process and to obtain a conceptual understanding of the adsorption mechanism associated with the phenomena.

The kinetics of gas uptake by the MWCNT at 288 K and about 14-15 bars were investigated (Fig. 6). The plots of q_t versus t showed that the adsorption kinetic of H_2 and CO_2 on MWCNT include of two steps, an initial rapid step where adsorption was fast and a second slow step where equilibrium uptake was obtained. The recorded data revealed a fast kinetics for the adsorption of H_2 and CO_2 in which most of adsorption occurs at early time of adsorption experiments and then adsorbent is saturated by the adsorbate. The initial high rate of gas uptake may be attributed to the existence of the vacant active sites and bare surface; however the number of available adsorption sites decreased as the number of gas molecules adsorbed increased. The equilibrium time was 9 min for H_2 and 24 min for CO_2 [28-31].

Thermodynamic Studies: In order to obtain a conceptual understanding of the adsorption mechanism associated with the phenomena, heat of adsorption was calculated. Heat of adsorption shows the enthalpy change before and after adsorption. Therefore, it is a measure of the strength of interaction between gas molecules and the surface of adsorbent. The isosteric heat of adsorption is defined by Clausius-Clapeyron equation [32, 33].

$$\Delta H_{st} = R \frac{d \ln p}{d\left(1/T\right)}\bigg|_{q_e} \qquad (4)$$

Where p (bar) is pressure at constant equilibrium uptake, R (J/mol.k) is the gas constant and T (K) is temperature. The plot of lnp versus 1/T gives the isosteric heat of adsorption (Fig. 8). A rule of thumb in adsorption is that heat of adsorption of 80 kJ/mol or more indicates chemisorption and smaller values is representative of physisorption [34, 35]. The obtained amounts of heat of adsorption for both gas much smaller than 80 kJ/mol. This indicates that the process of H_2 and CO_2 adsorption on the MWCNT used in this study is dominated by physisorption. The negative slopes are shown in Fig. 7 reconfirmed that the process of adsorption is exothermic.
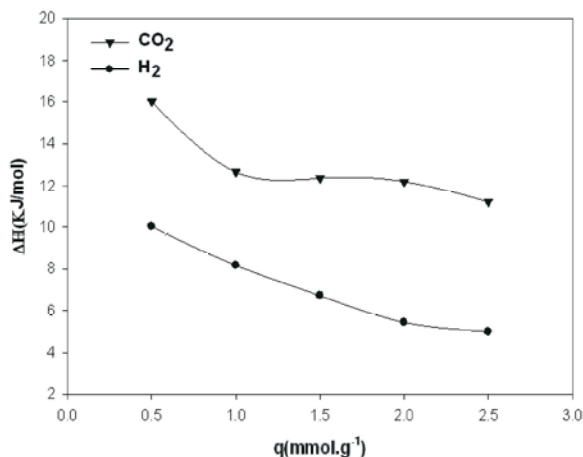

Fig. 8: Variation of the isosteric heat of adsorption with the amount of adsorbed H_2 and CO_2

Fig. 8 depicts the variation of the isosteric heat of adsorption with the amount of adsorbed H_2 and CO_2. By increasing surface coverage, the isosteric heat of adsorption of both gases decreases. This reality confirms that in lower pressure gas molecules can come into direct contact with the MWCNT. This causes a stronger interaction between gases and MWCNT. Therefore the isosteric heat of adsorption increases. The occupation of pores at higher gas equilibrium pressure causes the weak interaction between gases and MWCNT occur. Hence the adsorption enthalpy decreases. A comparison between the heat of adsorption of H_2 and CO_2 (Fig. 8) reveals that the heat of adsorption of CO_2 is higher than the heat of adsorption of H_2 on the surface coverage. The higher heat of sorption of CO_2 shows that CO_2 is adsorbed more strongly on MWCNT compared with H_2. Maybe because of this fact that the molecular mass of CO_2 is higher than H_2 this causes increasing Van-der Waals forces between gas molecules and adsorbent.

CONCLUSIONS

The equilibrium uptakes of H_2 and CO_2 by multi-walled carbon nanotube adsorbent were measured at temperature range of 288-318 K and pressure up to 40 bars. Describing the sorption equilibria by Langmuir and Freundlich models through a non linear fit to the experimental isotherm data confirmed the affinity between H_2 and CO_2 on MWCNT had an inverse relationship with temperature and indicating an exothermic reaction. The results emphasized that lower temperature and higher pressure is needed to improve the gas uptake by MWCNT. The kinetics of H_2 and CO_2 uptake at 288 K and 14-15 bars revealed a fast adsorption kinetics for both gases in which most of adsorption occurred at early time of adsorption experiments and then adsorbent was saturated by the adsorbate. Small values of isosteric heat of adsorption indicated physical nature of adsorption mechanism. In conclusion, the general results obtained from equilibrium, kinetic and thermodynamic studies indicated that MWCNTs is a promising adsorbent for CO_2 removal from flue gas (mixture of H_2 and CO_2).

REFERENCES

1. Dodziuk, H. and G. Dolgonos, 2002. Molecular modeling study of hydrogen storage in carbon nanotubes. Chemical Physics Letters, 356(1-2): 79-83.

2. Huang, W., X. Zhang, J. Tu, F. Kong, J. Ma, F. Liu, H. Lu and C. Chen, 2003. The effect of pretreatments on hydrogen adsorption of multi-walled carbon nanotubes. Materials Chemistry and Physics, 78(1): 144-148.

3. Cao, D. and J. Wu, 2005. Modeling the selectivity of activated carbons for efficient separation of hydrogen and carbon dioxide. Carbon, 43(7): 1364-1370.

4. Giunta, P., C. Mosquera, N. Amadeo and M. Laborde, 2007. Simulation of a hydrogen production and purification system for a PEM fuel-cell using bioethanol as raw material. J. Power Sources, 164(1): 336-343.

5. Brunetti, A., F. Scura, G. Barbieri and E. Drioli, 2010. Membrane technologies for CO_2 separation. J. Membrane Sci., 359(1-2): 115-125.

6. Olajire, A.A., 2010. CO_2 capture and separation technologies for end-of-pipe applications-A review. Energy, 35(6): 2610-2628.

7. Chatti, R., A.K. Bansiwal, J.A. Thote, V. Kumar, P. Jadhav, S.K. Lokhande, R.B. Biniwale, N.K. Labhsetwar and S.S. Rayalu, 2009. Amine loaded zeolites for carbon dioxide capture: Amine loading and adsorption studies. Microporous and Mesoporous Materials, 121(1-3): 84-89.

8. Chang, F.Y., K.J. Chao, H.H. Cheng and C.S. Tan, 2009. Adsorption of CO_2 onto amine-grafted mesoporous silicas. Separation and Purification Technol., 70(1): 87-95.

9. Zelenak, V., D. Halamova, L. Gaberova, E. Bloch and P. Llewellyn, 2008. Amine-modified SBA-12 mesoporous silica for carbon dioxide capture: Effect of amine basicity on sorption properties. Microporous and Mesoporous Materials, 116(1-3): 358-364.

10. Knofel, C., J. Descarpentries, A. Benzaouia, V. Zelenak, S. Mornet, P. Llewellyn and V. Hornebecq, 2007. Functionalised micro-/mesoporous silica for the adsorption of carbon dioxide. Microporous and Mesoporous Materials, 99(1-2): 79-85.

11. Pevida, C., M.G. Plaza, B. Arias, J. Fermoso, F. Rubiera and J.J. Pis, 2008. Surface modification of activated carbons for CO_2 capture. Applied Surface Sci., 254(22): 7165-7172.

12. Wei, J., L. Liao, Y. Xiao, P. Zhang and Y. Shi, 2010. Capture of carbon dioxide by amine-impregnated as-synthesized MCM-41. J. Environmental Sci., 22(10): 1558-1563.

13. Saha, D. and S. Deng, 2009. Enhanced hydrogen adsorption in ordered mesoporous carbon through clathrate formation. International J. Hydrogen Energy, 34(20): 8583-8588.

14. Huang, C.C., H.M. Chen and C.H. Chen, 2010. Hydrogen adsorption on modified activated carbon. International J. Hydrogen Energy, 35(7): 2777-2780.

15. Anson, A., M.A. Callejas, A.M. Benito, W.K. Maser, M. Izquierdo, B. Rubio, J. Jagiello, M. Thommes, J. Parra and M.T. Martinez, 2004. Hydrogen adsorption studies on single wall carbon nanotubes. Carbon, 42(7): 1243-1248.

16. Reddy, A.L.M. and S. Ramaprabhu, 2008. Hydrogen adsorption properties of single-walled carbon nanotube- Nanocrystalline platinum composites. International J. Hydrogen Energy, 33(3): 1028-1034.

17. Foroutan, M. and A.T. Nasrabadi, 2010. Adsorption behavior of ternary mixtures of noble gases inside single-walled carbon nanotube bundles. Chemical Physics Letters, 497(4-6): 213-217.

18. Fitzgerald, J., Z. Pan, M. Sudibandriyo, R. Robinson, K. Gasem and S. Reeves, 2005. Adsorption of methane, nitrogen, carbon dioxide and their mixtures on wet Tiffany Coal. Fuel, 84(18): 2351-2363.

19. Sheikh, M.A., M.M. Hassan and K.F. Loughlin, 1996. Adsorption equilibria and rate parameters for nitrogen and methane on Maxsorb activated carbon. Gas Separation and Purification, 10(3): 161-168.

20. Yulong, W., W. Fei, L. Guohua, N. Guoqing and Y. Mingde, 2008. Methane storage in multi-walled carbon nanotubes at the quantity of 80 g. Materials Research Bulletin, 43(6): 1431-1439.

21. Ioannatos, G.E. and X.E. Verykios, 2010. H_2 storage on single-and multi-walled carbon nanotubes. International J. Hydrogen Energy, 35(2): 622-628.

22. Sohn, S. and D. Kim, 2005. Modification of Langmuir isotherm in solution systems--definition and utilization of concentration dependent factor. Chemosphere, 58(1): 115-123.

23. Ghaemi, A., M. Torab-Mostaedi and M. Ghannadi-Maragheh, 2011. Characterizations of strontium (II) and barium (II) adsorption from aqueous solutions using dolomite powder. J. Hazardous Materials, 190(2): 916-921.

24. Hsueh, C.L., Y.W. Lu, C.C. Hung, Y.H. Huang and C.Y. Chen, 2007. Adsorption kinetic, thermodynamic and desorption studies of CI Reactive Black 5 on a novel photoassisted Fenton catalyst. Dyes and Pigments, 75(1): 130-135.

25. Rahchamani, J., H.Z. Mousavi and M. Behzad, 2011. Adsorption of methyl violet from aqueous solution by polyacrylamide as an adsorbent: Isotherm and kinetic studies. Desalination, 267(2): 256-260.

26. Hsueh, C.L., Y.W. Lu, C.C. Hung, Y.H. Huang and C.Y. Chen, 2007. Adsorption kinetic, thermodynamic and desorption studies of CI Reactive Black 5 on a novel photoassisted Fenton catalyst. Dyes and Pigments, 75(1): 130-135.

27. Fu, Q., Y. Deng, H. Li, J. Liu, H. Hu, S. Chen and T. Sa, 2009. Equilibrium, kinetic and thermodynamic studies on the adsorption of the toxins of Bacillus thuringiensis subsp. kurstaki by clay minerals. Applied Surface Sci., 255(8): 4551-4557.

28. Malkoc, E. and Y. Nuhoglu, 2007. Potential of tea factory waste for chromium (VI) removal from aqueous solutions: Thermodynamic and kinetic studies. Separation and Purification Technol., 54(3): 291-298.

29. Chen, S., Q. Yue, B. Gao, Q. Li and X. Xu, 2011. Removal of Cr (VI) from aqueous solution using modified corn stalks: Characteristic, equilibrium, kinetic and thermodynamic study. Chemical Engineering J., 168(2): 909-917.

30. Kamari, A. and W.S.W. Ngah, 2009. Isotherm, kinetic and thermodynamic studies of lead and copper uptake by H_2SO_4 modified chitosan. Colloids and Surfaces B: Biointerfaces, 73(2): 257-266.

31. Ahmaruzzaman, M. and S. Laxmi Gayatri, 2010. Batch adsorption of 4-nitrophenol by acid activated jute stick char: Equilibrium, kinetic and thermodynamic studies. Chemical Engineering J., 158(2): 173-180.

32. Hsu, S.C., C. Lu, F. Su, W. Zeng and W. Chen, 2010. Thermodynamics and regeneration studies of CO_2 adsorption on multiwalled carbon nanotubes. Chemical Engineering Sci., 65(4): 1354-1361.

33. Zhou, L., Y. Zhou and Y. Sun, 2004. A comparative study of hydrogen adsorption on superactivated carbon versus carbon nanotubes. International J. Hydrogen Energy, 29(5): 475-479.

34. Rodrigues, L.A. and M.L.C.P. Da Silva, 2010. Thermodynamic and kinetic investigations of phosphate adsorption onto hydrous niobium oxide prepared by homogeneous solution method. Desalination, 263(1-3): 29-35.

35. Cinke, M., J. Li, C.W. Bauschlicher, A. Ricca and M. Meyyappan, 2003. CO_2 adsorption in single-walled carbon nanotubes. Chemical Physics Letters, 376(5-6): 761-766.